https://doi.org/10.46813/2024-154-072

TWO STAGE HALL TYPE SOURCE: DISCHARGE CHARACTERISTICS AND ELECTRON ENERGY DISTRIBUTION FUNCTION

V.Yu. Bazhenov, A.M. Dobrovolskii, V.V. Tsiolko, V.M. Piun

Institute of Physics NAS of Ukraine, Kyiv, Ukraine

E-mail: tsiolko@iop.kiev.ua

The influence of working gas pressure and potentials of the cathodes of the two-stage plasma source with an anode layer on the dynamic current-voltage and power-voltage characteristics of separate stages of the discharge has been established. The effect of the source operating modes on the EEDF was determined by the method of emission optical diagnostics. In particular, the existence of a group of electrons with energy of ≈ 35…50 eV was found in the axial zone of the plasma source.

PACS: 52.65.-y, 52.25.Xz, 52.27.Aj

INTRODUCTION

Hall type plasma sources due to their simple design and high reliability of plasma generation in a wide range of conditions are widely used in science and technology, in particular in the creation of ion thruster for electric propulsion [1–3]. Sources of this type can have different designs, but all of them have the advantage of volumetric acceleration of ions from the ionization zone and the absence of output grids that should form an accelerated ion flow. One of the options for sources with a closed electron current are the sources with an anode layer (ALT). Previously, we created the ALT based source of a cylindrical plasma flow with its two-stage formation [4]. The source increases the efficiency of the volume usage. The peculiarity of the source is the ionization of the working gas in the anode layer on the periphery of the beam diameter, the accumulation of space charge in the main part of the volume of the beam formation and the formation of the beam itself by the space charge field. The source enables formation of two oppositely directed thrusts without change of the source position in the space. The peculiarity of the proposed design was the presence of two cathodes in the form of several rods that were located inside the anode symmetrically relative to the middle plane of the anode. If necessary, it was possible to change the currents through individual cathodes, thereby changing both the longitudinal and radial distributions of the plasma parameters. However, there is a problem of controlled selection of the thrust and control of the thrust energy independently of ion generating discharge.

For a source of small volume, one can use a compromise solution. The working gas should not be injected through the anode, but along the axis of the thrust flow formation. It also allows one to abandon the symmetrical scheme of the discharge gap between anode and two cathodes under the same potential and make the second cathode electrically independent. The appearance of the second independent cathode allows one to redistribute the power of the power source between the stages of the source and try to influence the energy of the thrust. The source design with two independent cathodes was considered in the paper [5]. Currents and potentials of the cathodes were defined by installing resistive loads in their circuits. The performed study shows the possibility of forming a large-diameter plasma flow in a source with separation of ionization zones and flow formation due to the accumulated space charge. The output current can reach up to 70% of the discharge current and depends on the discharge conditions. The obtained results also show the dependence of the flow formation on the potentials of the cathodes, which are electrically independent. This demonstrates the possibility of independent control of the energy of the ions in the flow regarding to the potential in the discharge with the anode layer. It was determined that the discharge in a gap between the anode and the cathodes exhibited two modes – low-current and high-current one. In the low-current mode, which existed only at pressures below a certain P_{thr}, the discharge plasma glow was observed in the form of a simultaneous glow near the surface of the anode and as a thin (diameter ~ 1 mm) spoke on the axis of the system. Variation of the discharge parameters resulted in changes of the distribution and character of the radiation emission from the volume.

To optimize the Hall type sources, it is important to understand the electron dynamics and the knowledge of the electron energy distribution function (EEDF). Electrons are the main charge carriers that close the discharge current and provide ionization of the working gas. For the existence of a volume charge in the volume of the formation of the thrust flow, it is also important that the recombination in this part of the source is minimal. EEDF studies by probe methods face great difficulties due to the presence of a strong magnetic field, the small internal volume of the source, and the complex geometry of the device. Changes in the distribution of radiation emission from the source volume with variation of power supplied to the discharge stages determined in [5] make it possible to use the methods of optical emission spectroscopy to evaluate changes in the EEDF depending on the redistribution of the supplied power and other changes in the existence of the working environment.

1. EXPERIMENTAL DEVICE AND DIAGNOSTICS

Schematic diagram of the experimental device is presented in Fig. 1. When conducting experimental studies, the pulse-periodic mode of operation of the power source was used. At that, the anode voltage looked as an each two seconds repeated sequence of four half-sine shaped pulses with 50 Hz power net frequency and 4.2 kV idle amplitude. A detailed description of the experimental setup and operation of the power source is presented in [5].

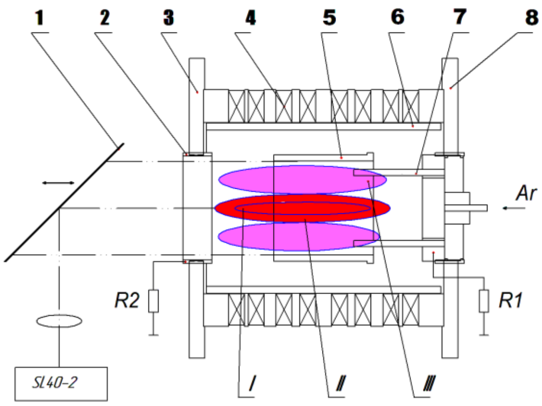

Fig. 1. Scheme of experimental device:
1 – movable mirror; 2 – external cathode C2;
3 – dielectric flanges; 4 – magnet system; 5 – anode;
6 – quartz cylinder; 7, 8 – internal cathode C1;
I, II, III – specific zones of the plasma glow

When studying the electro-physical characteristics of the discharge, measurements were made of voltages and currents of cathodes C1, C2 (U_{c1}, U_{c2}, I_{c1}, I_{c2}, respectively), anode voltage U_a, at different values of argon pressure and values of resistances R1, R2.

Plasma emission spectra were studied using a CCD spectrometer SL40-2-2048 in the wavelength range of 400…900 nm with a resolution of about 0.5 nm. The design of the optical system provided spatial scanning of the emission detection zone along the radius of cylindrically symmetric plasma device (see Fig. 1) by longitudinal move of the mirror 1 reflecting radiation at an angle of 90^0, while other elements of the optical system remained stationary. The radiation entered the spectrometer through an optical waveguide with an effective input diameter of about 0.4 mm. The projection of the radiation reception zone onto the entrance of the waveguide was carried out using a lens with a focal length of 105 mm and a relative aperture that could vary from 1:4.5 to 1:16. Note that even with the maximum aperture, the effective value was limited to about 1:8 due to the angular aperture of the waveguide. Such configuration was used in most studies, and only with very strong signals the relative aperture was reduced to 1:16. The length of the optical path from the lens to the center of the discharge system at the average position of the mirror was about 600 mm, which provided an effective diameter of the perception zone of about 2 mm with its effective length of about 100 mm for the correct measurement of transverse distributions inside the discharge area. The exposure time when recording the spectra was 0.1 s with a period of 2 s according to the discharge power mode. The speed of movement of the mirror was about 0.06 mm/s. The duration of the recording cycle of the spatial distribution was 20 min, and the resulting array of 600 spectra was stored in a file using the spectrometer software for further processing.

2. EXPERIMENTAL RESULTS

2.1. CURRENT-VOLTAGE AND POWER-VOLTAGE CHARACTERISTICS OF THE DISCHARGE STAGES

During the research, pulsed voltage from the power source was applied to the discharge anode relative to the grounded chamber. Cathodes C1, C2 were connected to the grounded chamber through resistors R1, R2 of different values. This made it possible to raise the potentials of the cathodes during the discharge glow to simulate the operation of the device in free space. Here are presented the results of studies of current-voltage and power-voltage characteristics (further noted as CVCs and PVCs, respectively) of the discharge stages measured in resistively loaded circuits of the cathodes C1 and C2. The studies were performed using resistances of 10 kΩ and 820 Ω in three options of their connection to the cathodes C1 and C2 (option I – R1 = 10 kΩ, R2 = 820 Ω; option II – R1 = 10 kΩ; option III = 820 Ω, R2 = 820 Ω).

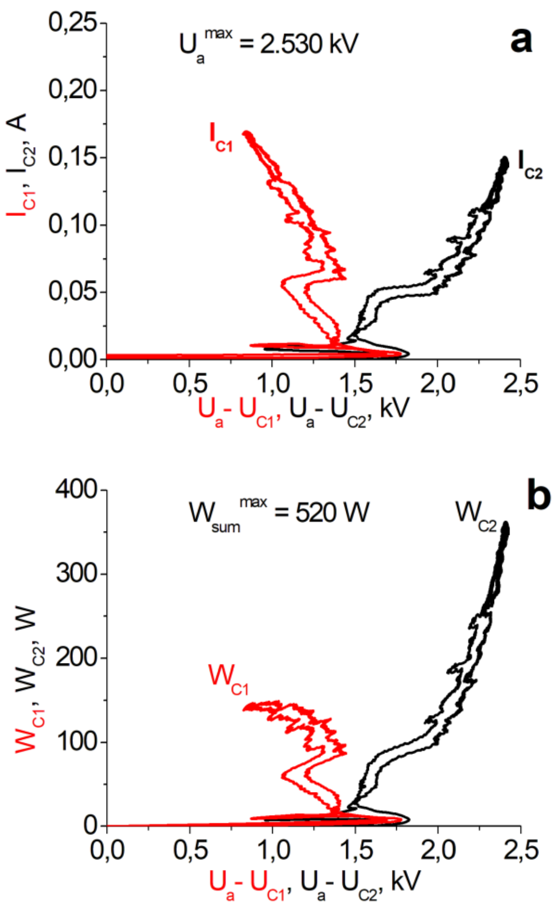

Fig. 2. Dynamic CVCs (a) and PVCs (b) of the discharge stages measured in C1 and C2 circuits. R1 = 10 kΩ, R2 = 820 Ω, P = 0.9·10^{-4} Torr

Fig. 2 presents dynamic CVCs and PVCs of the discharge stages in case of connecting the resistors by option I at argon pressure 0.9·10^{-4} Torr. One can see that the discharge at voltage $U_{ign} \approx 1.750$ kV is initially ignited in low-current mode (milliampere range) and subsequently switches to high-current mode. The behaviors of CVCs and PVCs of the discharge stages differ significantly from each other. If the discharge voltage U_a - U_{C2} and the current I_{C2} simultaneously increase and decrease synchronously with U_a, then the behavior of U_a - U_{C2} and I_{C1} is somewhat different - the increase in the current I_{C1} is accompanied by a decrease in the discharge voltage U_a - U_{C1} and vice versa. If the maximum values of the discharge currents I_{C1}, I_{C2} are almost close in magnitude, then the maximum power values supplied via the cathodes differ by ≈ 2.5 times. Moreover, the main power is supplied in the external discharge stage between the anode and cathode C2 ($W_{C2}^{max} \approx 350$ W).

An increase in argon pressure approximately three times from $0.9 \cdot 10^{-4}$ to $2.9 \cdot 10^{-4}$ Torr causes changes in the values of some discharge parameters, but does not fundamentally affect the of CVCs and PVCs behaviors for the discharge stages (see Fig. 2,a,b). In particular, an increase in argon pressure leads to a decrease in the ignition voltage U_{ign} from ≈ 1,750 to ≈ 1,250 kV, U_a^{max} from 2.530 to 1.910 kV (and, accordingly, the maximum values of the discharge voltages in particular discharge stages) and the total power W_{sum}^{max} to 450 W . However, the power supplied in the discharge stage between the anode and cathode C2 remains approximately the same $W_{C2}^{max} \approx 350$ W.

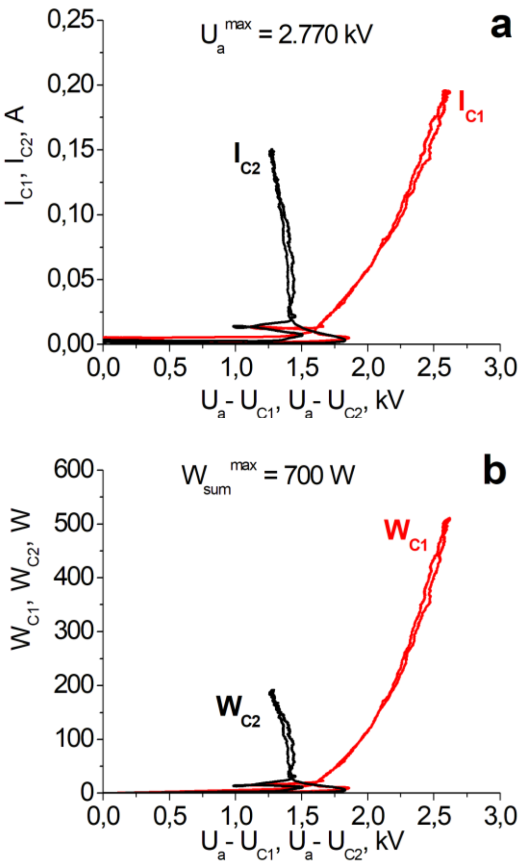

Fig. 3. Dynamic CVCs (a) and PVCs (b) of the discharge stages measured in C1 and C2 circuits. R1 = 820 Ω, R2 = 10 kΩ, P = $0.9 \cdot 10^{-4}$ Torr

The dynamic characteristics of the discharge obtained when connecting resistances by option II (R1 = 820 Ω, R2 = 10 kΩ) and an argon pressure of $0.9 \cdot 10^{-4}$ Torr are presented in Fig. 3. Comparison with Fig. 2 shows that when connecting resistors by option II, the redistribution of power between stages of the system changes. The maximum anode voltage U_a^{max} increases from 2.530 to 2.770 kV, and the value of the total maximum power in the discharge W_{sum}^{max} increases from 520 to 700 W. This increase in power occurs mainly due to the increase in maximum discharge voltages and the major portion of the power ($W_{C1}^{max} \approx 500$ W) is supplied in the internal stage between the anode and cathode C1.

An increase in the argon pressure to $2.9 \cdot 10^{-4}$ Torr leads to a drop in the anode voltage U_a^{max} from 2.770 to 2.020 kV and the total power in discharge stages W_{sum}^{max} to 460 W ($W_{C1}^{max} \approx 350$ W). This drop in the power value is primarily associated with a significant decrease in the maximum voltage values on the U_a - U_{C1} and U_a - U_{C2} discharge gaps.

In Fig. 4 CVCs and PVCs of the discharge stages obtained at argon pressure of $0.9 \cdot 10^{-4}$ Torr are presented for option III (symmetrical connection of 820 Ω resistors to cathodes C1, C2).

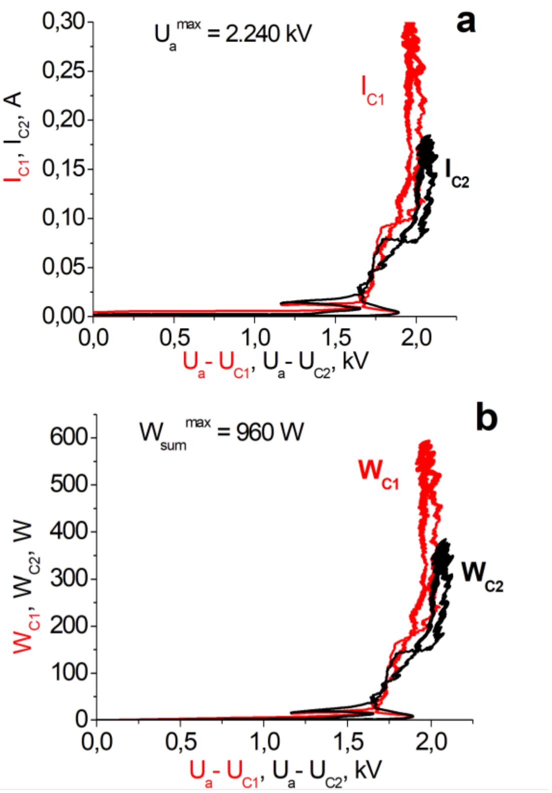

Fig. 4. Dynamic CVCs (a) and PVCs (b) of the discharge stages measured in C1 and C2 circuits. R1 = 820 Ω, R2 = 820 Ω, P = $0.9 \cdot 10^{-4}$ Torr

One can see from this figure that in this case the CVCs and PVCs for both stages are the same, except for the difference in the maximum values of I_{C1}, I_{C2}, W_{C1}^{max}, W_{C2}^{max}. With such a configuration of connecting the resistors, the maximum power

$W_{sum}^{max} \approx 960$ W is obtained, while a larger portion is supplied to the discharge through cathode C1 ($W_{C1}^{max} \approx 600$ W), and is determined primarily by the difference in currents $I_{C1}^{max}, I_{C2}^{max}$ (see Fig. 4,a).

Increasing the argon pressure to P = $2.9 \cdot 10^{-4}$ Torr leads to a decrease in both U_a^{max} to 1.770 kV and W_{sum}^{max} power to 720 W. At the same time, unlike the case of lower pressure, this power is divided equally between both stages of the discharge ($W_{C1}^{max} = W_{C2}^{max} \approx 360$ W).

Some integral characteristics of the source are summarized in Table.

Integral characteristics of the source

Option/ P, Torr	W_{sum}^{max}, W		U_a^{max}, kV	
	0.9e-4	2.9e-4	0.9e-4	2.9e-4
I	520	450	2.530	1.910
II	700	460	2.770	2.020
III	960	720	2.240	1.770

In general, one can see that the change in the argon pressure and the connection of various resistances to the cathodes C1, C2 in the three considered options significantly affects not only the total power consumed by the source, but also the power distribution between its discharge stages.

2.2. OPTICAL MEASUREMENTS

Let us consider how the parameters of the operating modes of the source affect the emission behavior of the argon lines ArI, λ = 750.39 nm (transition $2p_1 \rightarrow 1s_2$, E_{th} = 13.48 eV), ArI, λ = 811.53 nm, (transition $2p_9 \rightarrow 1s_5$, E_{th} = 13.08 eV) and several emission lines of singly ionized Ar II (data for these lines are taken from [6]).

The choice of these lines was determined by the following considerations. At an argon pressure of $< 10^{-3}$ Torr, the dominant mechanism in the occupation of the Ar ($2p_1$) level is excitation by an electron impact from the ground state, and the main part of the energy is emitted during the transition to the Ar($1s_2$) level [7]. The radiation intensity of the argon line is 750.39 nm $I_{750} \sim \sigma_{gr} n_g n_e f(\varepsilon)$ ($\varepsilon > 14$ eV), where: σ_g is excitation cross section of Ar ($2p_1$) level from the ground state; n_g, n_e are densities of Ar atoms in the ground state and in the plasma, respectively; f(ε) is electron energy distribution function. Thus, I_{750} is a certain measure of the plasma density and the content of electrons with energy greater than 14 eV.

Unlike the case of the previous line, the main channel for the population of the Ar($2p_9$) state is excitation by an electron impact from the metastable $1s_5$ states, despite the fact that in the plasma metastable atoms make up only a small fraction ~ ($10^{-5} \ldots 10^{-3}$) of argon atoms [8]. This is due to several factors. First, the value of the excitation cross section from the metastable level exceeds the value of the excitation cross section from the ground state by almost three orders of magnitude. Secondly, metastable atoms are already in an excited state, and only a small amount of additional energy (in this case $\varepsilon > 2$ eV) is needed to excite metastables to the $1p_9$ level (at the same time, to excite from the ground state of argon more than 13 eV is required). In a low-temperature plasma, the number of low-energy electrons with energy of several eV is orders of magnitude greater than the number of electrons with $\varepsilon > 13$ eV. Therefore, this combination of a large cross-section and low excitation threshold energy allows metastable atoms to play the main role in the excitation of the $1p_9$ level. That is, in other words, the radiation intensity of the 811.53 nm line $I_{811} \sim \sigma_m n_m n_e f(\varepsilon)$, (2 eV < ε < 15 eV), where: σ_m is excitation cross section of Ar($2p_9$) level from the metastable state Ar($1s_5$); n_m is density of metastable atoms. Knowing the intensity behavior of this line gives us information about the low-energy part of the EEDF.

Emission of ionized argon line Ar II λ = 487.98 nm (transition 4s $^2P_{3/2}$ - 4p $^2D^0_{5/2}$, E_{th} = 35.44 eV). This ArII line was chosen because its upper state is 20 eV above the ion state and 35 eV above the ground state of Ar. The maximum excitation crossing of this line is reached at electron energy of 50 eV. That is, the radiation of this line is evidence of the existence in the plasma of a group of fast electrons with energy ε ≈ 35…50 eV.

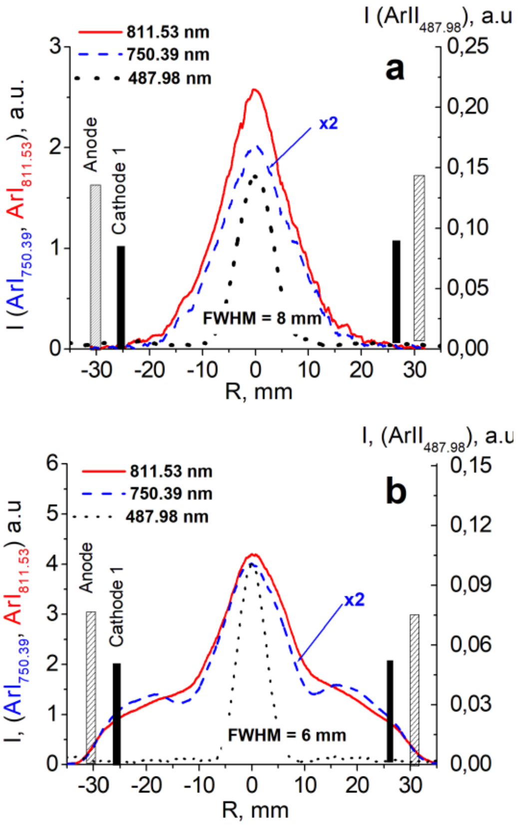

Fig. 5. Averaged over time and observation line radial dependences of intensities of the emission lines for atomic argon ArI (750.39 nm), ArI (811.53 nm) and atomic argon ion ArII (487.98 nm). R1 = 10 kΩ, R2 = 820 Ω. P = $0.9 \cdot 10^{-4}$ Torr (a), P = $2.9 \cdot 10^{-4}$ Torr (b)

When considering the obtained radial dependences of line intensities, it should be borne in mind that the obtained spectra are averaged not only over time, but also over the thickness of the discharge plasma L ≈ 100 mm. As mentioned above, different operating modes of the device are accompanied not only by changes in the total power, but also by a change in the distribution of this power between the discharge stages, that is, circuits of the cathodes C1, C2. That is, not only the average plasma density along the observation line, but also the longitudinal distribution of the plasma density changes in different regimes. All this affects, in particular, the nature of trapping radiation in the plasma. Therefore, on the basis of the obtained spectral data, only general conclusions can be drawn regarding the processes in the plasma.

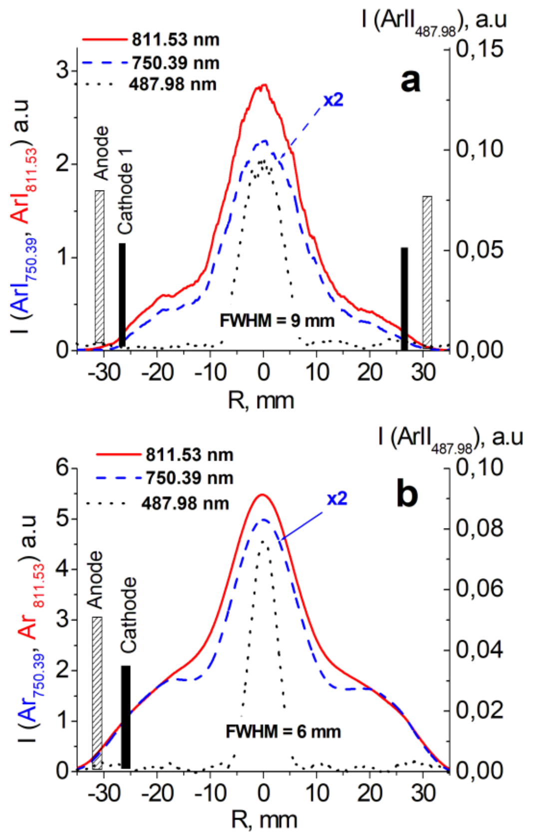

Fig. 6. Averaged over time and observation line radial dependences of intensities of the emission lines for atomic argon ArI (750.39 nm), ArI (811.53 nm) and atomic argon ion ArII (487.98 nm).
R1 = 820 Ω, R2 = 10 kΩ.
P = 0.9·10⁻⁴ Torr (a), P = 2.9·10⁻⁴ Torr (b)

At low argon pressure, in the case of connecting resistances R1, R2 according to option I, the radiation inside the device has the form of a rod with a diameter of about 20 mm (see zone II in Fig. 1), surrounded by plasma with a much lower brightness. Blue radiation in the form of a thin cord is observed throughout zone II of the glow in the axial region (zone I in Fig. 1). The radial dependences of the radiation intensity of the lines ArI (750.39 nm), ArI (811.53 nm) practically coincide and have a bell-shaped form (Fig. 5,a). The central part (core) with the temperature of electrons with energy greater than ≈ 35 eV is much narrower – the FWHM of ArII radiation at a wavelength of 487.98 nm is 8 mm. An increase in the argon pressure causes a decrease in the value of W_{sum}^{max} by only ≈ 15% (see text above) with a simultaneous (see Fig. 5,b) increase in the radiation intensity of the ArI lines on the axis of the system by approximately 1.5–2 times and the appearance of “wings” (see zone III, Fig. 1) on their radial distributions. At the same time, an increase in pressure leads to a decrease in the intensity of the ArII line and the FWHM of its generation zone.

Changes of the radial intensity profiles of the ArI lines are primarily related to the reconstruction of the spatial structure of the discharge. As the pressure/density of argon increases, an increase in plasma brightness is visually observed in the near-anode zone, followed by the spread of this glow to the axis of the system. Therefore, the radial distribution of the intensity of the Ar I lines represents a superposition of the glow of the central plasma rod and the tubular plasma that surrounds this rod. The smoother profile of the radial distribution of Ar(811.53) radiation is due to the fact that electrically neutral metastable atoms can freely diffuse across the magnetic field.

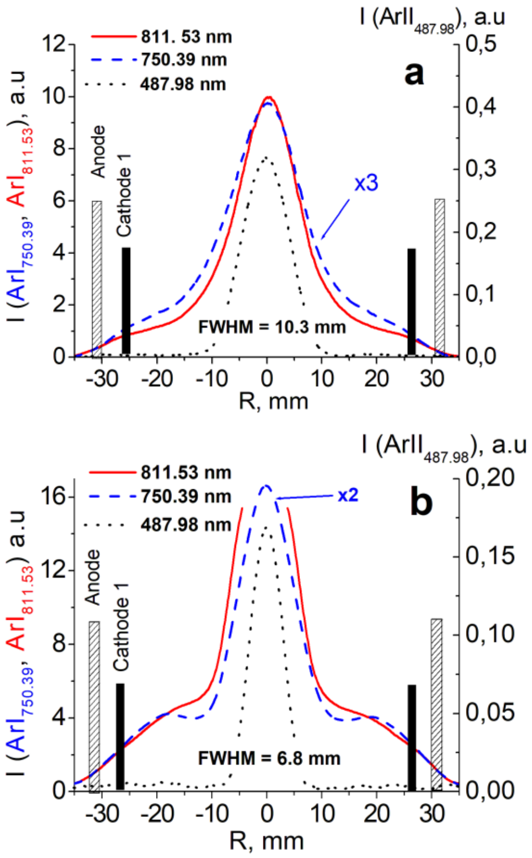

Fig. 7. Averaged over time and observation line radial dependences of intensities of the emission lines for atomic argon ArI (750.39 nm), ArI (811.53 nm) and atomic argon ion ArII (487.98 nm).
R1 = 820 Ω, R2 = 820 Ω.
P = 0.9·10⁻⁴ Torr (a), P = 2.9·10⁻⁴ Torr (b)

The increase in the emission intensity of the ArI lines with increasing pressure is mainly related to both the increase in the density of argon atoms and the "cooling" of plasma electrons due to collisions (the latter, in particular, is evidenced by the decrease in the intensity of the ArII(487.98) line). The average plasma density along the length of the device changes slightly (because it depends on the power W_{sum}^{max}), so this “cooling” causes changes in the shape of f(ε) in the energy range ≈ 2…25 eV, which ultimately causes an increase in the degree of population of $1p_1$ $1p_9$ levels.

Although the connection of resistors R1, R2 according to option II at low pressure causes an increase in the power W_{sum}^{max} from 520 to 700 W, but this does not lead to significant changes in the radiation intensity of lines ArI, ArII. in the axial region, just only to appearance of "wings" on their radial distribution (Fig. 6).

An increase in pressure is accompanied by the same changes in the behavior of the radial distribution of the intensity of ArI, ArII lines as in the case of Option I: an increase in the intensity of the Ar(750.39), Ar(811.53) lines both in the axial region and in the "wings" of their radial distributions; decrease in the intensity of the ArII(487.98) line and the FWHM of the spatial zone of its generation. Some difference in the intensity of the lines may be related to the fact that in the case of Option II, the main energy is supplied to the discharge through the C1 cathode.

Unlike the case of the transition from Option I to Option II at low pressure, in the case of transition to Option III, the increase in power W_{sum}^{max} from 700 to 960 W is accompanied by an increase in the intensity of lines ArI, ArII in the axial region by almost three times (Fig. 7). The reasons for this difference in behavior are currently not fully understood.

An increase in argon pressure with a simultaneous decrease in power, as in the previous cases, leads to an increase in the intensity of the Ar(750.39), Ar(811.53) lines (in the latter case, the signal amplitude was limited by the dynamic range of the spectrometer) both in the axial region and and in the "wings" of their radial distributions and to decrease the intensity of the ArII(487.98) line and the FWHM of the spatial zone of its generation.

SUMMARY

The obtained results provide an understanding of the peculiarities of the change in EEDF shape of the source plasma depending on the modes of its operation. They show the formation in the near-axis volume of a significant number of "hot" electrons with energies from 14 to 50 eV. This can explain the ability of the system to accumulate ions despite the existence of a large number of slower electrons in the volume. Interesting is the existence of this group of "hot electrons" in all investigated operating modes of the source.

As the measurements show, the number of electrons capable of ionizing the working gas is very significant throughout the volume of the plasma source. In the discharge gap of the first stage, the efficiency of ionization is also increased due to the magnetic field, which significantly increases the lifetime of ionizing electrons with energy greater than ≈ 15 eV.

REFERENCES

1. I. Levchenko, S. Xu, S. Mazouffre, F. Taccogna, and K. Bazaka. Perspectives, frontiers, and new horizons for plasma-based space electric propulsion // *Phys. Plasmas.* 2020, p. 020601. Doi: 10.1063/1.5109141
2. K. Holste, P. Dietz, S. Scharmann, et al. Ion thrusters for electric propulsion: Scientific issues developing a niche technology into a game changer // *Rev. Sci. Instrum. 91*. 2020, p. 061101. DOI: 10.1063/5.0010134
3. O.I. Girka, K.I. Lee, Y.S. Choi, S.O. Jang. Ion beam figuring with focused anode layer thruster // *Rev Sci Instrum.* 2022, p. 063304. DOI: 10.1063/5.0071800
4. I. Litovko, A. Goncharov, A. Dobrovolskyi, and I. Naiko. The Emerging Field Trends Erosion-Free Electric Hall Thrusters Systems // *Plasma Science and Technology /* Edited by Aamir Shahzad, InTechOpen, London, 2022, Chapter 11, p. 195-214. DOI: 10.5772/intechopen.99096
5. V.Yu. Bazhenov, A.M. Dobrovolskiy, V.V. Tsiolko, V.M. Piun. Two stage plasma source for large scale beam generation // *Problems of Atomic Science and Technology. Series "Plasma Electronics and New Methods of Acceleration".* 2023, № 4, p. 121-124. DOI:10.46813/2023-146-121
6. John B. Boffard, B. Chiaro, Tobin Webwr, Cnun C. Lin. Electron impact excitation of argon: Optical emission cross section in the range of 300…2500 nm // *Atomic Data and Nuclear Data Tables.* 2007, v. 93, p. 831-863. DOI: 10.1016/j.adt.2007.06.004
7. John B. Boffard, R.O. Jung, Chun C. Lin, A.E. Wendl. Optical emission measurements of electron energy distributions in low-pressure argon inductively coupled plasmas // *Plasma Sources Sci. Technol.* 2010, v. 19, p. 065001. DOI: 10.1088/0963-0252/19/6/065001
8. John B. Boffard, Garrett A. Piech, Mark F. Gehrke, L.W. Anderson, and Chun C. Lin. Measurement of electron-impact excitation cross section out of metastable levels of argon and comparison with ground state excitation. *// Phys. Rev*. 1999, A 59, p. 2749. DOI: 10.1103/PhysRevA.59.2749

Article received 15.10.2024

ДВОСТУПЕНЕВЕ ДЖЕРЕЛО ХОЛЛІВСЬКОГО ТИПУ: ХАРАКТЕРИСТИКИ РОЗРЯДУ ТА ФУНКЦІЯ РОЗПОДІЛУ ЕЛЕКТРОНІВ ПО ЕНЕРГІЯХ

В.Ю. Баженов, А.М. Добровольський, В.В. Ціолко, В.М. Піун

Встановлено вплив тиску робочого газу та потенціалів катодів двоступеневого плазмового джерела з анодним шаром на динамічні вольт-амперні та ват-амперні характеристики окремих ступенів розряду. Методами емісійної оптичної діагностики встановлено вплив режимів роботи джерела на ФРЕЕ. Зокрема було знайдено існування в приосьовій зоні плазми джерела групи електронів з енергією ≈ 35…50 еВ.